AD-A060 789 BOEING COMMERCIAL AIRPLANE CO SEATTLE WASH F/G 20/4
NONLINEAR INTERACTION BETWEEN MEAN AND UNSTEADY FLOWFIELDS NEAR--ETC(U)
1978 W C CHIN N00014-78-C-0349
UNCLASSIFIED NL

1 OF 1
AD
A060789

END
DATE FILMED
1-79
DDC

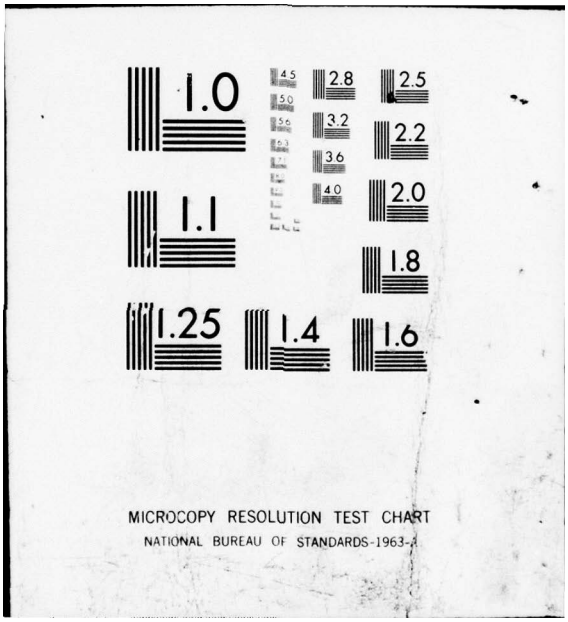
1.0
1.1
1.25
1.4
1.6
1.8
2.0
2.2
2.5
2.8
3.2
3.6
4.0
4.5
5.0
5.6
6.3
7.1
MICROCOPY RESOLUTION TEST CHART
NATIONAL BUREAU OF STANDARDS-1963-A

LEVEL II

NONLINEAR INTERACTION BETWEEN MEAN AND UNSTEADY FLOWFIELDS NEAR MACH 1

Contract N00014-78-C-0349

by Wilson C. Chin*

Boeing Commercial Airplane Company

Seattle, Wash.

*Specialist Engineer, Aerodynamics Research Group, Member AIAA.

Index Categories: Subsonic and Transonic Flow; Nonsteady Aerodynamics.

12 29 p. 15 N00014-78-C-0349

ABSTRACT

The nonlinear interaction between a steady transonic mean flow and that induced by superposed small-amplitude oscillations is studied using the method of harmonic expansions. A truncated system of spectral equations is derived which accounts for both frequency and amplitude dependent changes to the mean flow, as would be induced by Reynolds stress feedback, and in particular, that owing to the primary harmonics. A three-level mixed-differencing scheme, conservative to leading order, is devised to solve for the nonlinearly coupled mean and unsteady disturbance flows. Calculations are performed for the NACA 64A006 airfoil with an aft-mounted quarter chord oscillating flap, for a range of subcritical and supercritical Mach numbers, reduced frequencies, and flap deflection angles. The results are compared with existing linear and nonlinear computations, and with some experimental results of Tijdeman; also, for flap-type oscillations, the nonlinear response of the mean flow to growing unsteady perturbations can be described in qualitative terms, and given simple physical explanation. At least for the cases considered,

390 145

the results of numerical experiments suggest that the nonlinear back-interaction on the mean flow, anticipated especially for low reduced frequencies, is insignificant even for "large amplitude" oscillations; also, the response of the unsteady loading to changes in flap deflection angle appears to be a linear one. The effects of nonlinearity, however, are important to the extent that unrealistic overpredictions in leading edge perturbation pressure, as obtained from linear finite difference calculations, and which persist even at very high subsonic freestream Mach numbers, are significantly reduced. The nonlinear coupling therefore restrains the influence of upstream propagating or "receding" waves that do not actually belong in the physical problem. Calculations were carried up to the point of Ehlers' so-called "Helmholtz divergence", beyond which uncontrolled numerical instabilities were encountered. The harmonic method presented here is not as computationally efficient as existing ADI methods, for example, the recent scheme of Ballhaus and Goorjian, but it does yield some insight into the governing dynamical processes, and it may be useful in nonlinear flutter analyses.

I. INTRODUCTION

Consider a two-dimensional airfoil in a subsonic freestream executing small-amplitude harmonic oscillations about a mean disturbance flow. Let x,y and t be streamwise, transverse and time coordinates, respectively, γ be the ratio of specific heats, and characterize the nonoscillating part of the unsteady configuration by a maximum thickness h and a chord c. Furthermore, let M_∞, U_∞, ρ_∞ and P_∞ denote the freestream values of Mach number, streamwise velocity, fluid density, and static pressure. The steady transonic limit refers to $\tau \to 0$ and $M_\infty \to 1$, where $\tau = h/c$ is the thickness ratio, and the similarity parameter $K = (1 - M_\infty^2)/\tau^{2/3}$ is held

fixed. This idea is extendable to unsteady flows. For sufficiently slow temporal variations, the nondimensional variables $\tilde{x} = x/c$, $\tilde{y} = \tau^{1/3} y/c$ and $\tilde{t} = \tau^{2/3} U_\infty t/c$ are of order unity, and the asymptotic expansion $\Phi = U_\infty \{x + c\tau^{2/3} \varphi(\tilde{x},\tilde{y},\tilde{t}) + \ldots\}$ for the total velocity potential Φ yields, to leading order, the perturbation potential equation

$$\{K-(\gamma+1)\varphi_{\tilde{x}}\}\varphi_{\tilde{x}\tilde{x}} + \varphi_{\tilde{y}\tilde{y}} - 2\varphi_{\tilde{x}\tilde{t}} = 0 \qquad (1)$$

In the same low-frequency approximation, when $y = \tau c F(\tilde{x},\tilde{t})$ represents the unsteady airfoil displacement, we have the tangency condition

$$\varphi_{\tilde{y}}(\tilde{x},0,\tilde{t}) = F_{\tilde{x}}(\tilde{x},\tilde{t}) \qquad (2)$$

consistently applied on the slit $\tilde{y} = 0$. The pressure coefficient C_p measures deviations of the local static pressure P from P_∞, and is obtained from

$$C_p = \frac{P-P_\infty}{\frac{1}{2}\rho_\infty U_\infty^2} \cong -2\tau^{2/3}\varphi_{\tilde{x}}(\tilde{x},\tilde{y},\tilde{t}) \qquad (3)$$

The Kutta condition, applied on the downstream slit emanating from the trailing edge, insists on pressure continuity, and requires that the jump

$$[\varphi_{\tilde{x}}] = \varphi_{\tilde{x}}(\tilde{x},0+,\tilde{t}) - \varphi_{\tilde{x}}(\tilde{x},0-,\tilde{t}) \qquad (4)$$

identically vanish across the wake; thus, $[\varphi]$ is a function of time only, and is instantaneously equal to the potential jump at the trailing edge. To Eqs. (2) and (4) we add, of course, regularity conditions for the

mean flow, and radiation conditions for the unsteady disturbance flow, but in a form suitable for convenient numerical implementation.

With airfoil motions that are harmonic in time and which, primarily, are small unsteady oscillations about a steady disturbance flow, it is plausible to linearize the unsteady problem about a steady flow, where the latter may be taken to be the solution for the nonoscillating airfoil. This idea was first given in Landahl[1,2] although, at the time, the extent to which Landahl's suggestion held true could not be assessed. Successful computational methods for mixed-type boundary value problems admitting shocked solutions have only become available recently. In 1971, Murman and Cole[3] successfully calculated mixed flows with embedded shockwaves using a "type-dependent" relaxation method; their scheme, for nonlifting flows, was extended to lifting configurations in Krupp and Murman[4], and was further improved to allow for the proper conservative capture of flow discontinuities in Murman[5]. These investigations have established the computational feasibility for practical transonic flow calculations. The calculation of unsteady flows, as suggested in Landahl's linearized formulation, is also amenable to type-differencing techniques. Ehlers[6] and Traci, Albano, Farr and Cheng[7], for example, have independently computed the unsteady field induced by small, unsteady oscillations using, as input to Landahl's variable coefficients, the steady background flow as obtained from Murman's algorithm (in both of these studies, the problem is Fourier-transformed in time, as will be the case in the present paper). The foregoing cited references form the basis of modern transonic flow calculations.

In linearized theory, the nonlinear mean flow is obtained once from a Murman-Cole method, and its solution fixes the variable coefficients of a linear, frequency-dependent, mixed-type problem. This linearization,

however, is not strictly correct: the nonharmonic part of the total disturbance flow must change for different disturbance frequencies and amplitudes because the physical problem is inherently nonlinear. The mean flow cannot be regarded as completely fixed for all time; the "ε-expansion" (that is, the straightforward linearization) breaks down because the nonlinear feedback, which arises from the usual harmonic interplay, and which builds up over the initial transient period during which the oscillations commence, is not described.

This back-interaction effect, generally assumed to be $O(\varepsilon^2)$, where ε characterizes the smallness of the unsteady oscillation amplitude relative to, say, the thickness of the mean geometry, is ignored in linear theory. For many practical applications, linear theory more or less suffices; however, for low-frequency transonic flows, generally associated with large aerodynamic loadings as well as large unsteady shock excursions, the neglect of nonlinear feedback may well be incorrect. Thus, one might anticipate that those formally $O(\varepsilon^2)$ terms may, in fact, be large: they may have a significant effect on the actual mean shock location and strength, and hence, on the unsteady perturbation field (for high frequencies, the effect is probably less pronounced, and a linearized approach should do). To describe this back-interaction, the nonlinear coupling between mean and disturbance flows must be retained, and new expansions must be introduced to reflect the parametric dependence of the actual flutter problem on the freestream Mach number, the oscillation frequency ω, and the oscillation amplitude ε, given some airfoil section. In essence: the ε-expansion may not retain its uniform validity over the entire range of ω's. The present study explores the consequences of nonlinearity for the well documented NACA 64A006 airfoil.

II. ANALYSIS

To implement the ideas discussed in the Introduction, expand the disturbance potnetial φ in the real series

$$\varphi(\tilde{x},\tilde{y},\tilde{t}) = \varphi_0(\tilde{x},\tilde{y}) + \tfrac{1}{2}\varepsilon(\varphi_1 e^{i\omega\tilde{t}} + \bar{\varphi}_1 e^{-i\omega\tilde{t}}) + \dots \tag{5}$$

where $\bar{\varphi}_1(x,y)$ is the complex conjugate of φ_1, and higher harmonic terms are not shown. Linearized unsteady theory defines a sequence of problems by equating coefficients of like powers of ε (the φ_0 problem, of course, is nonlinear). This, as previously stated, is not always correct because the nonharmonic mean flow is rendered independent of ε and ω, and this is physically unrealizable. To remedy this defect, a sequential ordering is instead introduced by equating coefficients of like harmonics. The resulting equations, if they can be accurately solved, involve no approximations and describe the physical problem exactly. However, since they are infinite in number, some type of truncation is needed. This is possible if $\varepsilon \ll 1$; for then, it is likely that higher harmonics, associated with high-order amplitude effects, can be neglected. We therefore retain in the mean flow equation only those "feedback" terms arising from the primary harmonics. Hence, the expansions

$$\begin{aligned}\varphi(\tilde{x},\tilde{y},\tilde{t}) &\cong \varphi_0(\tilde{x},\tilde{y}) + \tfrac{1}{2}\varepsilon(\varphi_1 e^{i\omega\tilde{t}} + \bar{\varphi}_1 e^{-i\omega\tilde{t}}) \\ &= \varphi_0(\tilde{x},\tilde{y}) + \varepsilon(\varphi_1^r \cos\omega\tilde{t} - \varphi_1^i \sin\omega\tilde{t})\end{aligned} \tag{6}$$

and

$$\begin{aligned}F(\tilde{x},\tilde{t}) &\cong f(\tilde{x}) + \tfrac{1}{2}\varepsilon\{g(\tilde{x})e^{i\omega\tilde{t}} + \bar{g}(\tilde{x})e^{-i\omega\tilde{t}}\} \\ &= f(\tilde{x}) + \varepsilon(g^r \cos\omega\tilde{t} - g^i \sin\omega\tilde{t})\end{aligned} \tag{7}$$

where $\varphi_1 = \varphi_1^r + i\,\varphi_1^i$ and $g = g^r + ig^i$, in the usual notation, lead to three coupled nonlinear boundary value problems, namely, for the mean flow,

$$\{K-(\gamma+1)\varphi_{o\tilde{x}}\}\,\varphi_{o\tilde{x}\tilde{x}} + \varphi_{o\tilde{y}\tilde{y}} = \frac{\varepsilon^2(\gamma+1)}{2}\{\varphi_{1\tilde{x}}^r\varphi_{1\tilde{x}\tilde{x}}^r + \varphi_{1\tilde{x}}^i\varphi_{1\tilde{x}\tilde{x}}^i\} \tag{8}$$

$$\varphi_{o\tilde{y}}(\tilde{x}, 0\pm) = f_{\tilde{x}}^{\pm}(\tilde{x}) \quad \text{on the chord} \tag{9}$$

$$[\varphi_{o\tilde{x}}] = 0 \quad \text{on the wake} \tag{10}$$

for the φ_1^r flow,

$$\{K-(\gamma+1)\varphi_{o\tilde{x}}\}\,\varphi_{1\tilde{x}\tilde{x}}^r - (\gamma+1)\,\varphi_{o\tilde{x}\tilde{x}}\varphi_{1\tilde{x}}^r + \varphi_{1\tilde{y}\tilde{y}}^r = -2\omega\,\varphi_{1\tilde{x}}^i \tag{11}$$

$$\varphi_{1\tilde{y}}^r(\tilde{x}, 0\pm) = g_{\tilde{x}}^{r\,\pm}(\tilde{x}) \quad \text{on the chord} \tag{12}$$

$$[\varphi_{1\tilde{x}}^r] = 0 \quad \text{on the wake} \tag{13}$$

and, for the φ_1^i flow,

$$\{K-(\gamma+1)\varphi_{o\tilde{x}}\}\,\varphi_{1\tilde{x}\tilde{x}}^i - (\gamma+1)\,\varphi_{o\tilde{x}\tilde{x}}\varphi_{1\tilde{x}}^i + \varphi_{1\tilde{y}\tilde{y}}^i = 2\omega\,\varphi_{1\tilde{x}}^r \tag{14}$$

$$\varphi_{1\tilde{y}}^i(\tilde{x}, 0\pm) = g_{\tilde{x}}^{i\,\pm}(\tilde{x}) \quad \text{on the chord} \tag{15}$$

$$[\varphi_{1\tilde{x}}^i] = 0 \quad \text{on the wake} \tag{16}$$

The ideas underlying the foregoing expansions were first described in Chin[8], where the expanded forms for the corresponding jump conditions may be found. These are suited for shock-fitting analyses, but the overall

complexity of the total formulation forbids rigorous numerical analysis; thus, a plausible "shock-capturing" algorithm, which ignores the internal boundary defined by the evolving shockwave, is used.

III. NUMERICAL PROCEDURE

A column relaxation scheme employing mixed-differencing and tridiagonal matrices is used which sweeps the computation box from upstream to downstream. The field variables φ_0, φ_1^r and φ_1^i are first initialized to zero. Eqs. (8-10) for the mean potential φ_0 are first solved by "sweeping" the flowfield once, with φ_1 "frozen"; then, Eqs. (11-13) are solved, again sweeping through once, with φ_0 and φ_1^i frozen, and finally, φ_1^i is solved using Eqs. (14-16), with φ_0 and φ_1^r fixed. This triple-sweep operational sequence defines one "iteration". The latest available values of φ_0 and φ_1 are always used to evaluate the coefficient and "right side" arrays, effectively linearizing the solution along each line. It is not clear how to construct a strictly conservative scheme. One needs to generalize Murman's[5] derivation for the steady shock-point operator for unsteadiness, using the somewhat cumbersome jump conditions in Chin[8], and this has so far proved unwieldy.

Conservative schemes for the steady, lifting problem are readily available. In computing the mean flow, the $O(\varepsilon^2)$ right side of Eq. (8), which represents unsteady Reynolds stress effects, is assumed to be a known prescribed forcing function. Murman's conservative differencing is implemented through Jameson's[9] convenient "switching function" formulation. For example, if $\Delta\tilde{x}$ and $\Delta\tilde{y}$ are constant nonvariable mesh widths in the streamwise and transverse directions, respectively, whose relative positions

are indicated by the indices i and j, and if

$$A_{i,j} = K\ -(\gamma+1)\ \frac{\varphi_{i+1,j} - \varphi_{i-1,j}}{2\,\Delta\tilde{x}}\ ,$$

$$P_{i,j} = A_{i,j}\ \frac{\varphi_{i+1,j} - 2\,\varphi_{i,j} + \varphi_{i-1,j}}{(\Delta\tilde{x})^2}\ ,$$

$$q_{i,j} = \frac{\varphi_{i,j+1} - 2\varphi_{i,j} + \varphi_{i,j-1}}{(\Delta\tilde{y})^2}\ ,\ \text{and}$$

$$S_{i,j} = \begin{cases} 0 \text{ if } A_{i,j} > 0 \\ 1 \text{ if } A_{i,j} < 0 \end{cases}\ ,$$

a fully conservative approximation to Eq. (8), conserving mass across the evolving shock is, with errors of $O(\varepsilon^2)$, $(1 - S_{i,j})P_{i,j} + S_{i-1,j}P_{i-1,j} + q_{i,j} = RHS_{i,j}$, where $RHS_{i,j}$ denotes the right hand side of Eq. (8). This difference equation is solved through column relaxation, as suggested by the regrouping

$$\varphi_{i,j-1} + \left\{-2(1-S_{i,j})A_{i,j}\left(\frac{\Delta\tilde{y}}{\Delta\tilde{x}}\right)^2 + S_{i-1,j}A_{i-1,j}\left(\frac{\Delta\tilde{y}}{\Delta\tilde{x}}\right)^2 - 2\right\}\varphi_{i,j} + \varphi_{i,j+1}$$

$$= -(1-S_{i,j})A_{i,j}\left(\frac{\Delta\tilde{y}}{\Delta\tilde{x}}\right)^2\varphi_{i+1,j}$$

$$-\left\{(1-S_{i,j})A_{i,j}\left(\frac{\Delta\tilde{y}}{\Delta\tilde{x}}\right)^2 - 2\,S_{i-1,j}A_{i-1,j}\left(\frac{\Delta\tilde{y}}{\Delta\tilde{x}}\right)^2\right\}\varphi_{i-1,j}$$

$$-S_{i-1,j}A_{i-1,j}\left(\frac{\Delta\tilde{y}}{\Delta\tilde{x}}\right)^2\varphi_{i-2,j} + (\Delta\tilde{y})^2\,RHS_{i,j}$$

The airfoil tangency condition and the wake Kutta condition are handled in the manner of Krupp and Murman[4], taking due account of the $RHS_{i,j}$ array, and the farfield boundaries defined by the computation box are updated at the end of each sweep. The tridiagonal equations obtained along each column are linearized about "old" values, and the columns are solved successively from upstream to downstream. The details of this algorithm are straightfowardly implemented.

For the perturbation flows φ_1^r and φ_1^i we proceed in a similar manner. The construction of proper shock-point and parabolic operators, in the sense of Murman[5], proved unwieldy. Thus, Murman and Cole's[3] original type-switching was employed, and this was implemented together with Ehlers'[6] treatment of unsteady tangency conditions and some simplified farfield boundary conditions of Seebass (to be described later). The unsteady solution for φ_1, therefore, is not fully conservative, although the mean flow solution is, to leading order. The sequential solution for φ_1^r and then φ_1^i completes the corrector level of the triple-sweep iteration, at which point the mean potential is once again solved. Both unsteady Kutta conditions are implemented as in Ref. 4.

On convergence of the relaxation, calculation of the surface pressure coefficient

$$C_p \cong -2\tau^{2/3}\varphi_{0_{\tilde{x}}} - 2\tau^{2/3}\varepsilon\left(\varphi_{1_{\tilde{x}}}^r \cos\omega\tilde{t} - \varphi_{1_{\tilde{x}}}^i \sin\omega\tilde{t}\right) \tag{17}$$

proceeds by streamwise differentiation of linearly extrapolated surface potentials. The definition

$$\begin{aligned} C_p &= C_{p_0} + \tfrac{1}{2}\varepsilon\left(C_{p_1} e^{i\omega\tilde{t}} + \overline{C_{p_1}}\, e^{-i\omega\tilde{t}}\right) \\ &= C_{p_0} + \varepsilon\left(C_{p_1}^r \cos\omega\tilde{t} - C_{p_1}^i \sin\omega\tilde{t}\right) \end{aligned} \tag{18}$$

is especially convenient. Our subsequent results will thus be expressed in terms of the functions $C_{p_0} = -2\tau^{2/3}\varphi_{0_{\tilde{x}}}$, $C^r_{p_1} = -2\tau^{2/3}\varphi^r_{1_{\tilde{x}}}$, and $C^i_{p_1} = -2\tau^{2/3}\varphi^i_{1_{\tilde{x}}}$. Note that ε is assumed to be proportional to the amplitude of the unsteady oscillation, e.g., the flap deflection, so that the functions $C^r_{p_1}$ and $C^i_{p_1}$, as defined, should remain nearly invariant throughout a range of sufficiently small ε's, as would be the case in linear theory.

IV. CALCULATED RESULTS

All of the results reported here were obtained on nonvariable meshes consisting of 80 grids in the streamwise direction, with twenty over the chord, and 60 grids in the transverse direction. Both $\Delta\tilde{x}$ and $\Delta\tilde{y}$, and supersonic and subsonic relaxation parameters, implemented as in Traci et al[7], were varied from case to case to provide stability and to ensure rapid convergence although, of course, in runs designed to test the effect of changing a single parameter, the same convergence parameters were assigned. For simplicity, in the unsteady problem, farfield boundary conditions calling for $\varphi_{1_{\tilde{x}}} = 0$ downstream and $\varphi_1 = 0$ elsewhere, as in Ballhaus and Goorjian[10] and Fung, Yu and Seebass[11], were used. The algorithm devised here is expensive and slowly convergent; typically, 1000 iterations are necessary to produce residuals of $O(10^{-4})$, although results sufficiently accurate for engineering applications can be obtained, to within 10% error, in 200 or so iterations. The present algorithm also suffers from Ehlers'[6] so-called "Helmholtz divergence" (see also Reference 7): nonconvergence occurs for sufficiently high freestream Mach numbers M_∞ and/or reduced frequencies k based on semichord. Of course, the present work concerns itself with low

frequency flows, and the latter constraint is not very significant; however, the former restriction on very supercritical flows prevents us from considering those severe cases for which large shock oscillations are anticipated. Nevertheless, the effects of nonlinearity, even for high subsonic and mildly supercritical flows, are of engineering and mathematical interest: how significant is the Reynolds stress feedback?

To answer this question, the flow about the NACA 64A006 airfoil with an aft-mounted quarter chord oscillating flap was studied. In particular, we considered the parameter ranges $0.80 \leq M_\infty \leq 0.85$ and $0.00 \leq k \leq 0.25$ (the $M_\infty = 0.85$, $k = 0.25$ case was the maximum nondivergent parameter set possible for the grid sizes and relaxation factors used), and flap deflection angles $\delta = 1^0$, 2^0 and 3^0. This run portfolio is especially useful since comparison with existing linear results and experimental data is possible. All of the calculations reported in this paper assume an unpitched mean geometry. We examine first several results for a flap deflection of $\delta = 1^0$, and a freestream Mach number of $M_\infty = 0.80$. The effects of increasing reduced frequency, shown in Figures 1, 2 and 3, correspond to $k = 0.0$, 0.064 and 0.25. All of the mean surface pressure coefficients obtained are identical to within 0.5%, and fall between the coarse mesh and fine mesh results of Traci et al. Good experimental correlation is also obtained. The unsteady force coefficients, in the convention of Ehlers[6], Traci[7] and Tijdeman[13,14,15], are expressed in terms of cross-chord jumps in $\mathcal{C}_p^{r,i} = \varepsilon C_{p_1}^{r,i} / \delta$, that is, in terms of $\Delta\mathcal{C}_p^{r,i}$. In all three figures, the hingeline $\Delta\mathcal{C}_p^{r}$ is well predicted by the nonlinear method. Leading edge results, however, are far from satisfactory. For example, in calculating $\Delta\mathcal{C}_p^{r}$, the linear finite difference methods of Ehlers and Traci both appear nearly singular while, on

the other hand, the magnitudes are underpredicted by the present theory. The exact reasons for the observed discrepancies are unclear. Certainly, on physical grounds, the effects of unsteady pressures ahead of the hinge axis should be minimal for high enough Mach numbers; this casts some doubt on the results of linear theory, and in this respect, nonlinear theory may represent a needed improvement. The effect of leading edge bluntness, too, was tested by modeling the infinite slope in separate runs using different "large" values, but the overall qualitative results for $\Delta C_p^{r,i}$ were unchanged from those presented here. It should be noted, however, that the present results correlated somewhat better with experimental data corresponding to higher Mach numbers (all of the calculations reported here assume an unbounded freestream, whereas Tijdeman's experiments were conducted in a porous wall wind tunnel). Figure 4, for $M_\infty = 0.825$ and $k = 0.0$, is to be compared with Figure 1; Figure 5 repeats the calculation of Figure 2, except that $M_\infty = 0.825$. Again, the same qualitative differences between linear and nonlinear results are evident. Agreement between the linear finite element results of Chan and Brashears[16] and the present results in Figure 2 appears to be fortuitous.

Figure 6 considers $M_\infty = 0.85$ and $k = 0.24$, again with $\delta = 1^o$. The mean pressure coefficient agrees moderately well with experiment. The unsteady peak pressure coefficients are predicted, and the qualitative shapes of the loading curves agree somewhat with wind tunnel data. The experimental results shown, as well as the (dashed) results of an unsteady linear calculation, are taken from Tijdeman[13].

Figures 7 and 8 deal with the question of increased flap deflections. The results for $M_\infty = 0.85$, $k = 0.24$ and $\delta = 1^o$, given in Figure 6, are replotted on the upper level of Figure 7, here in terms of C_{p_0}, $C_{p_1}^i$ and

$C^r_{p_1}$. Below each of these curves are the corresponding computed changes that would arise from increases in flap deflection, relative to the results for $\delta = 1^o$. For example, below the C_{p_0} curve for $\delta = 1^o$, the plots for $C_{p_0}(\delta=2^o) - C_{p_0}(\delta=1^o)$ and $C_{p_0}(\delta=3^o) - C_{p_0}(\delta=1^o)$ are given, and so on. The curves for <u>mean</u> flow are particularly interesting. For flap-type oscillations, an increase in flap deflection angle is seen to induce an underexpansion upstream of midchord and downstream of the hingeline, while in $0.5 \lesssim \tilde{x} \lesssim 0.75$, approximately, the flow overexpands. This same character is evident from Figure 8, which considers $M_\infty = 0.80$ and $k = 0.064$ (both the reduced frequency and the freestream Mach number here are reduced relative to their levels in Figure 7). However, in all of these cases, the changes to the C_{p_0} that would have been obtained on the static nonoscillating airfoil are probably insignificant in comparison with changes, say, that would arise out of changes to the computational parameters. For the unsteady flow, the $\delta = 3^o$ corrections (relative to the $\delta = 1^o$ results) are approximately twice those for $\delta = 2^o$, suggesting near-linearity. This is confirmed by the overall smallness of the correction magnitudes: changes in C_{p_1} with respect to changes in δ are almost negligible, although in some isolated cases, 5% differences can be found near the mean shock location and near the hinge line. Note that the mean $C^*_{p_0}$ level, shown in Figures 7 and 8, is defined from $K - (\gamma+1)\mathcal{P}_{\tilde{x}} = 0$. Further increases in M_∞ or k beyond those values used in Figure 7 gave rise to uncontrollable instabilities of the "Helmholtz" type. The question of linearity will be further reviewed in the next section, in light of experimental results.

V. DISCUSSION AND SUMMARY

When the present study first suggested itself, the aim was to demonstrate the predominance of nonlinear feedback, especially for those critical instances characterized by high freestream Mach numbers, low reduced frequencies, or large flap deflection angles. At least for the examples considered, however, the back-interaction on the mean flow has been a weak effect. The foregoing results suggest, in fact, that linearity holds and remains applicable over a fairly large range of M_∞, k and δ. This agrees with some tentative conclusions of Fung, Yu and Seebass[11]. The near-linearity of the unsteady problem is also consistent with results obtained by Magnus and Yoshihara[12] for the thicker NACA 64A410 airfoil, oscillating in pitch at Mach 0.72 and at various frequencies. These latter authors found that, even for this very supercritical flow, pressures at given locations and integrated quantities, such as normal force and pitching moments, responded sinusoidally in general; noticeably nonsinusoidal behaviour in the aft shock surface pressure was observed, however, for one very low frequency case.

A second indication of near-linearity is seen from Tijdeman's[13] experiments. For the NACA 64A006 airfoil at zero pitch and zero mean flap deflection angle, Tijdeman reports that "the mean steady pressure distributions correspond reasonably well with the steady pressure distributions ... obtained on the nonoscillating model" (these observations were based on a flap deflection of 1^0, with $k = 0.25$ and $0.80 \leq M_\infty \leq 0.94$). The question of linearity, pursued in this paper, was also explored by Tijdeman. Tests were conducted to establish the range of possible maximum flap deflection amplitudes over which a linear relationship existed between δ and the resulting unsteady loading. Linearity was established, but unfortunately, due to limitations in

the particular test set-up, only amplitudes up to 1^{o} were considered. On an experimental basis alone, Tijdeman's results are, of course, inconclusive: for small deflection amplitudes, the buffer furnished by the unsteady boundary layer reduces flap effectivity, so that the extent of "inviscid nonlinearity" cannot be truly assessed. The calculations reported in Figures 7 and 8, however, do support Tijdeman's conclusion; these results, purely inviscid in nature, were carried up to 3^{o}, and establish beyond doubt the linearity of the unsteady response. In this light, linearity appears to be meaningful in a transonic field; the experiments of Tijdeman and Zwaan[14], one might further note, also give a shock movement nearly proportional to the flap deflection for a sizeable range of flap angles.

This is not to say that nonlinearity is unimportant. Tijdeman[13] notes that "above $M_{\infty} = 0.875$, the measured unsteady pressures in front of the shock wave decrease strongly, and at $M_{\infty} = 0.94$, they are zero ahead of the hinge axis." On the other hand, both of the existing linear finite difference methods[6,7] give contrasting results. For example, Traci et al[7] observed that in both subcritical and supercritical cases, the pressure perturbations over the forward portion of the airfoil ($\tilde{x} \leq 0.75$) are consistently overpredicted; this is true even in their $M_{\infty} = 0.94$ test case, the calculated results showing a small but almost uniform pressure perturbation over the forward airfoil surface, whereas Tijdeman's results, which are consistent with the physics, indicate negligible effects. Traci attributes the observed discrepancies to real fluid effects and, perhaps, to numerical inconsistencies in the implementation of farfield boundary conditions. Although these are distinct possibilities, the global influence of the nonlinear coupling, retained in the present analysis, cannot be discounted. Various checks on

the numerical procedure have ruled out spurious effects tied to, say, coding technique or leading edge modeling. Thus, it seems that the added nonlinear coupling serves to restrain the influences of upstream-propagating or "receding" waves when they truly do not belong in the physical picture. This restraining effect, as is apparent from Figures 1-5, reduces the perturbation pressure level of linear theory, and leads to somewhat of an underprediction. Much of this remains speculative; for example, the reasons for the differences between linear finite difference and linear finite element models are still unclear. But it may be that, although the unsteady response to changes in deflection amplitude is linear, the exact pressure magnitudes must be obtained using a nonlinear theory. A similar situation arises in Whitham's sonic boom theory; there, the linear equation is valid, provided the "nonlinearly corrected" characteristics are used in the farfield.

In obtaining the results of Figures 7 and 8, extreme caution was exercised to assure that calculated differences in surface pressure for various deflection angles, which are small, are larger than changes that would be obtained, say, from iteration to iteration. For consistency, in each of Figures 7 and 8, results are presented at the same converged iteration number. The near-constancy of the mean flow to changes in δ and k, as obtained in these runs, does not, of course, imply that this is always the case; in fact, the time-marching ADI scheme of Ballhaus and Goorjian[10], using the small disturbance formulation, has successfully modeled all of Tijdeman's[13] unsteady flow configurations, namely, the so-called Type A, B and C shock motions. It does suggest, however, that truly nonlinear effects, at least for the NACA 64A006 airfoil, are probably confined to high subsonic Mach numbers very, very close to unity.

No attempt has been made at obtaining quantitative agreement with experiment. Experimental uncertainties (e.g., shock wave-boundary layer interaction, local separation, turbulence and wall interference), together with computational shortcomings, especially in the numerical treatment of leading edge expansions over blunt noses, make any "agreement" fortuitous. Accurate and meaningful comparisons with other numerical work are also difficult; differences in mesh definition, choice of relaxation parameters, implementation of farfield boundary conditions, and specification of mean flowfields (e.g., both References 6 and 7 use a nonconservative $\varphi_0(\tilde{x},\tilde{y})$) contribute to the basic problem. Perhaps the most pressing issue is the need to model real fluid effects accurately. Some headway has been made in the pioneering work of Magnus and Yoshihara[12], however, but clearly, much more work needs to be done.

Although the nonlinear harmonic method appears to give improved results over a wider range of flow parameters, a practical limitation on the approach is Ehlers'[6] "Helmholtz divergence" boundary, beyond which uncontrollable numerical instabilities arise. Until this problem is overcome, harmonic approaches are likely to be of limited usefulness in transonic computations. Of course, the present method was never intended for routine use, but rather, to assess the extent to which linear theory can model a nonlinear problem. Efficient time-marching schemes, such as the finite difference ADI method of Ballhaus and Goorjian[10], treat the nonlinear shock motion correctly and account for higher harmonic generation. The present work points to the need to develope accurate nonlinear models.

ACKNOWLEDGMENTS

This research was supported by the Office of Naval Research, and was monitored by Mr. Morton Cooper.

August 25, 1978

REFERENCES

1. Landahl, M.T., Unsteady Transonic Flow, International Series of Monographs in Aeronautics and Astronautics, Pergamon Press, London, 1961.
2. Landahl, M.T., "Linearized Theory for Unsteady Transonic Flow", in Symposium Transsonicum, edited by K. Oswatitsch, Springer-Verlag, Berlin, 1964, pp. 414-439.
3. Murman, E.M. and Cole, J.D., "Calculation of Plane Steady Transonic Flows", AIAA Journal, Vol. 9, No. 1, Jan. 1971, pp. 114-121.
4. Krupp, J.A. and Murman, E.M., "Computation of Transonic Flows Past Lifting Airfoils and Slender Bodies", AIAA Journal, Vol. 10, July 1972, pp. 880-886.
5. Murman, E.M., "Analysis of Embedded Shock Waves Calculated by Relaxation Methods", AIAA Journal, Vol. 12, No. 5, May 1974, pp. 626-633.
6. Ehlers, F.E., "A Finite Difference Method for the Solution of the Transonic Flow Around Harmonically Oscillating Wings", NASA CR-2257, Jan. 1974.
7. Traci, R.M., Albano, E.D., Farr, J.L., and Cheng, H.K., "Small Disturbance Transonic Flows About Oscillating Airfoils", AFFDL-TR-74-37, June 1974.
8. Chin, W.C., "Nonlinear Formulation for Low-Frequency Transonic Flow", AIAA Journal, Vol. 16, No. 6, June 1978, pp. 616-618.
9. Jameson, A., "Numerical Computation of Transonic Flows with Shock Waves", in Symposium Transsonicum II, edited by K.Oswatitsch and D. Rues, Springer-Verlag, Berlin, 1976, pp. 384-414.
10. Ballhaus, W.F. and Goorjian, P.M., "Implicit Finite Difference Computations of Unsteady Transonic Flows About Airfoils, Including the Treatment of Irregular Shock Wave Motions", AIAA Paper No. 77-205, presented at the AIAA 15th Aerospace Sciences Meeting, Los Angeles, Calif., January 1977.

11. Fung, K.Y., Yu, N.J., and Seebass, A.R., "Small Unsteady Perturbations in Transonic Flows", AIAA Paper No. 77-675, presented at the AIAA 10th Fluid and Plasmadynamics Conference, Albuquerque, New Mexico, June 1977.

12. Magnus, R.J. and Yoshihara, H., "Calculations of Transonic Flow Over an Oscillating Airfoil", AIAA Paper No. 75-98, presented at the AIAA 13th Aerospace Sciences Meeting, Pasadena, Calif., January 1975.

13. Tijdeman, H., "Investigations of the Transonic Flow Around Oscillating Airfoils", NLR-TR-77090-U, National Aerospace Laboratory, The Netherlands, 1977.

14. Tijdeman, H. and Zwaan, R.J., "On the Prediction of Aerodynamic Loads on Oscillating Wings in Transonic Flow", AGARD Report No. 612, 1974.

15. Tijdeman, H. and Schippers, P., "Results of Pressure Measurements on an Airfoil with Oscillating Flap in Two-Dimensional Flow (Zero Incidence and Zero Mean Flap Position)", NLR-TR-73078-U, National Aerospace Laboratory, The Netherlands, 1973.

16. Chan, S.T.K. and Brashears, M.R., "Finite Element Analysis of Unsteady Transonic Flow", AIAA Paper No. 75-875, presented at the AIAA 8th Fluid and Plasmadynamics Conference, Hartford, Connecticut, June 1975.

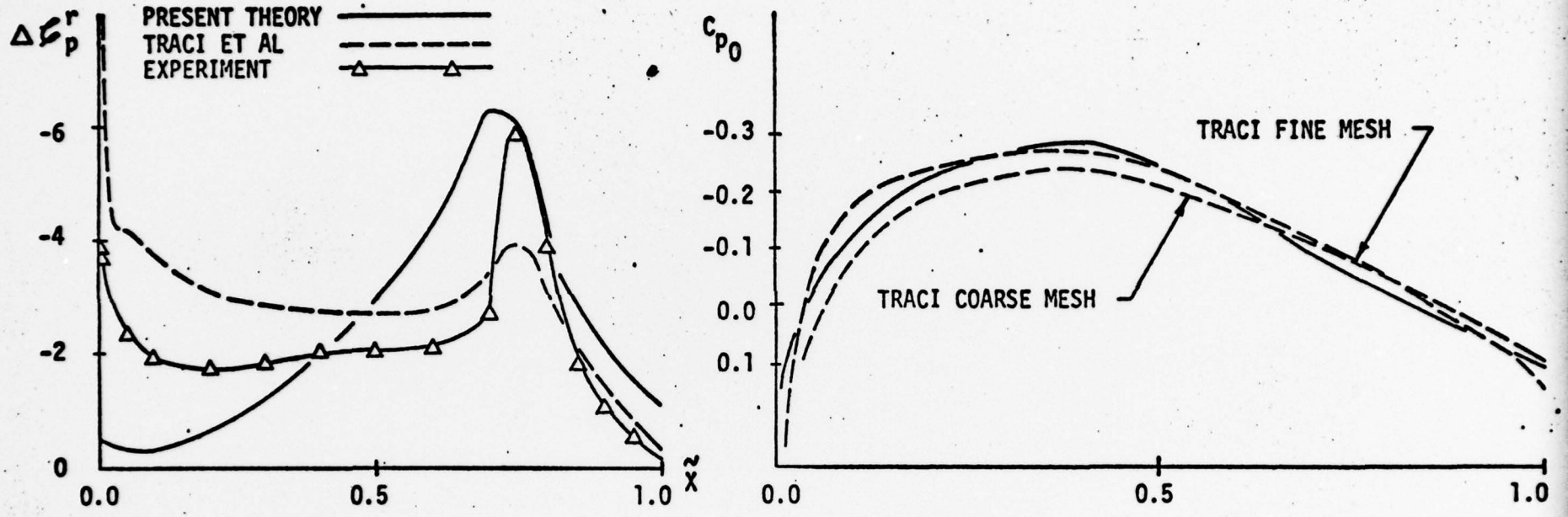

FIGURE 1. MACH 0.80, REDUCED FREQUENCY 0.00, FLAP DEFLECTION 1^o CASE.

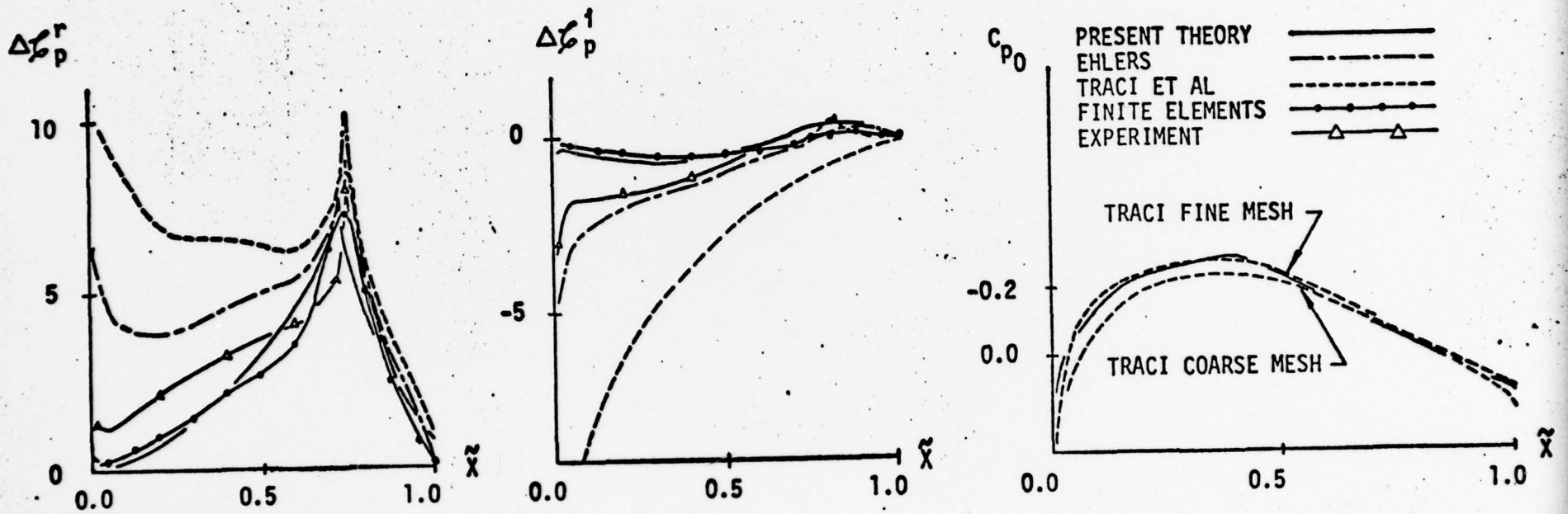

FIGURE 2. MACH 0.80, REDUCED FREQUENCY 0.064, FLAP DEFLECTION 1° CASE.

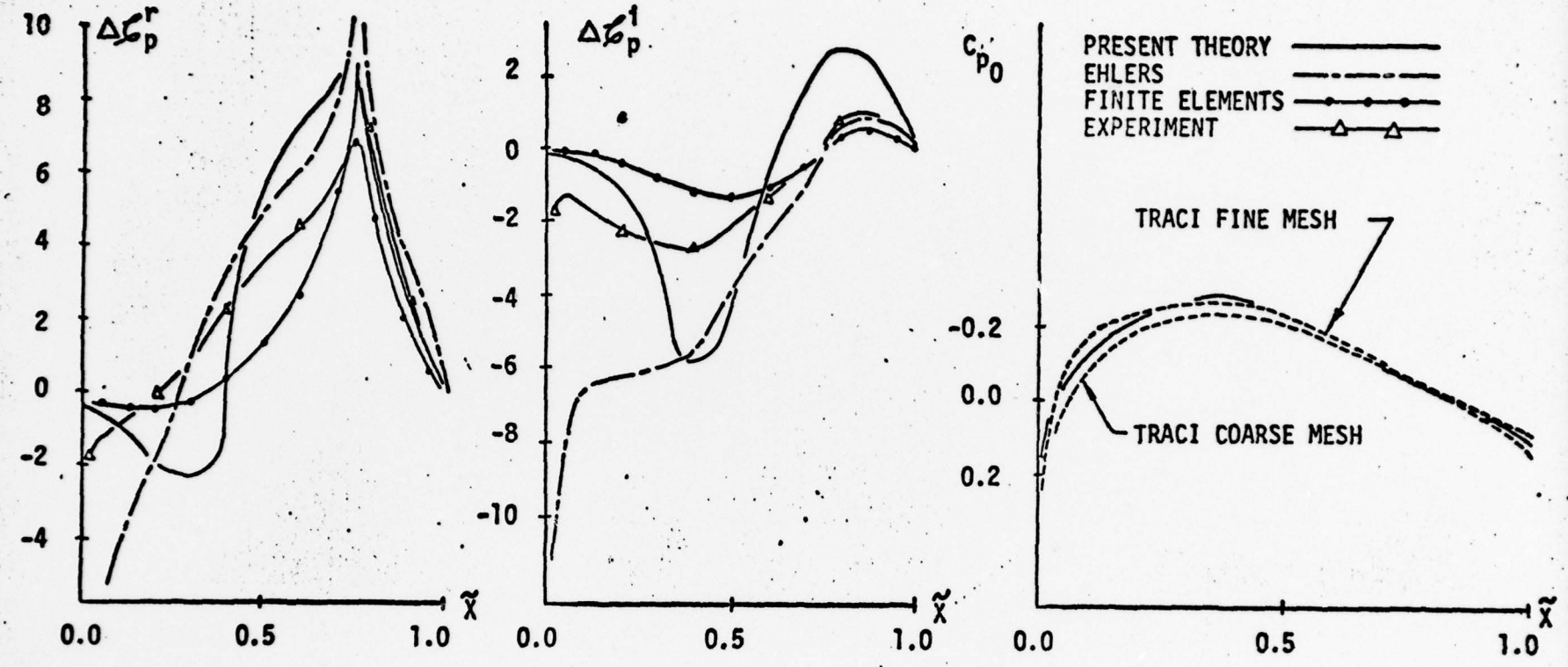

FIGURE 3. MACH 0.80, REDUCED FREQUENCY 0.25, FLAP DEFLECTION 1^o CASE.

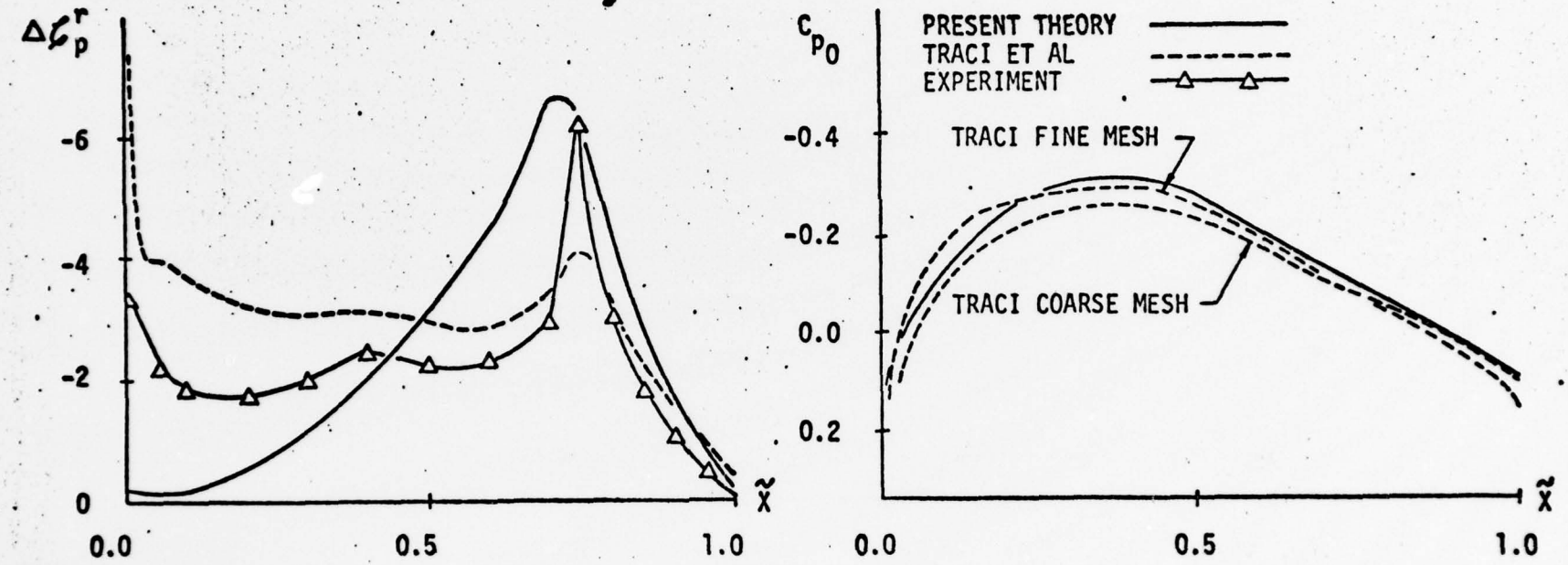

FIGURE 4. MACH 0.825, REDUCED FREQUENCY 0.00, FLAP DEFLECTION 1^o CASE.

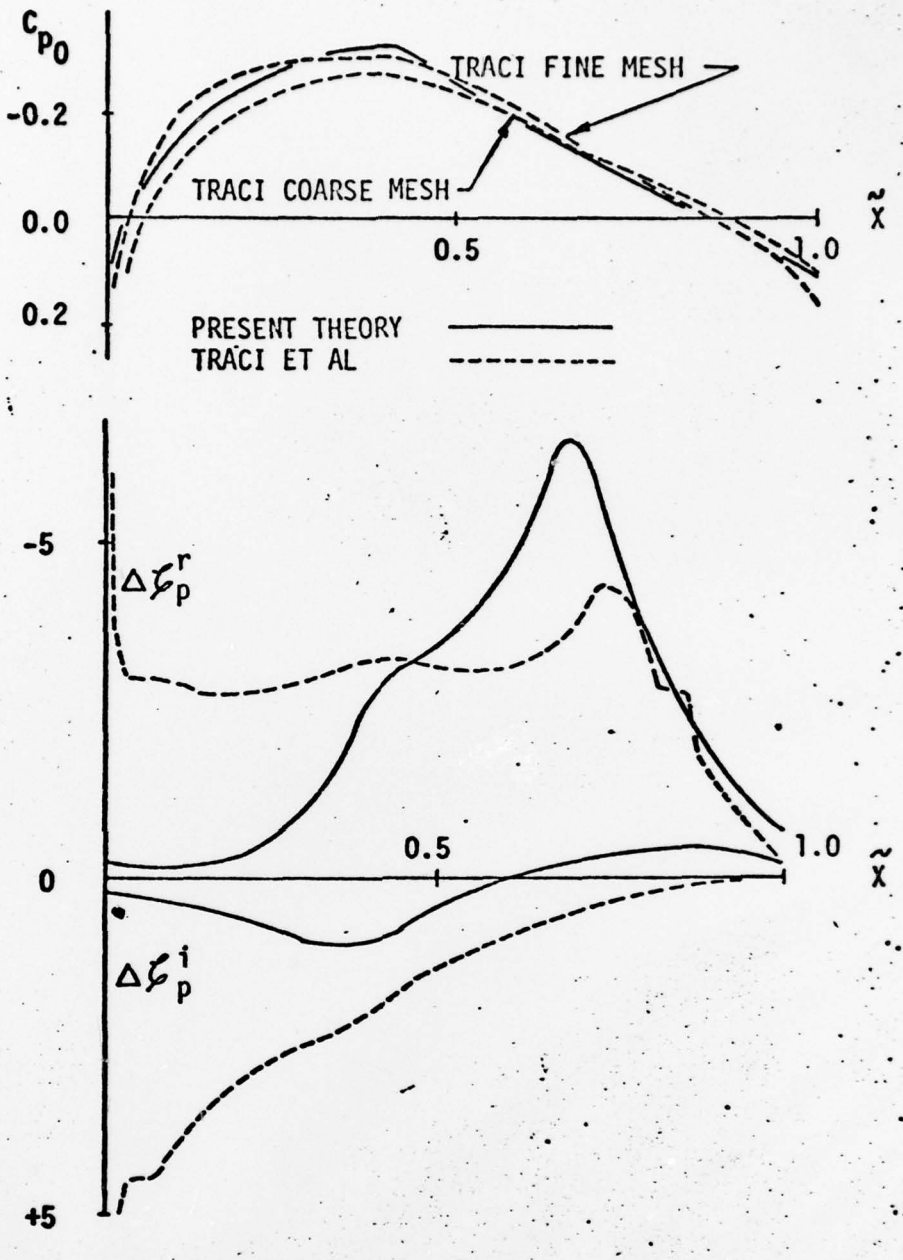

FIGURE 5. MACH 0.825, REDUCED FREQUENCY 0.064, FLAP DEFLECTION 1^o CASE.

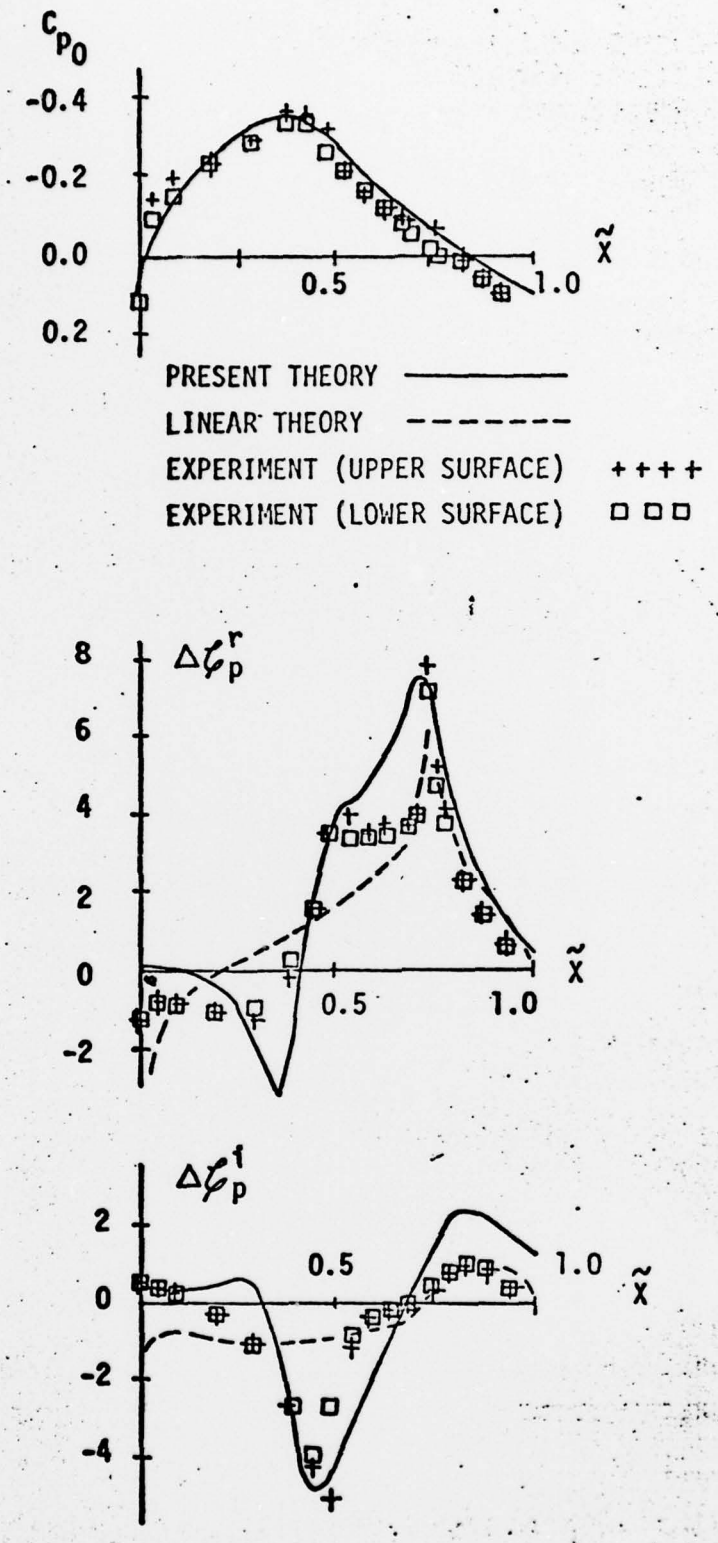

FIGURE 6. MACH 0.85, REDUCED FREQUENCY 0.24, FLAP DEFLECTION 1^o CASE.

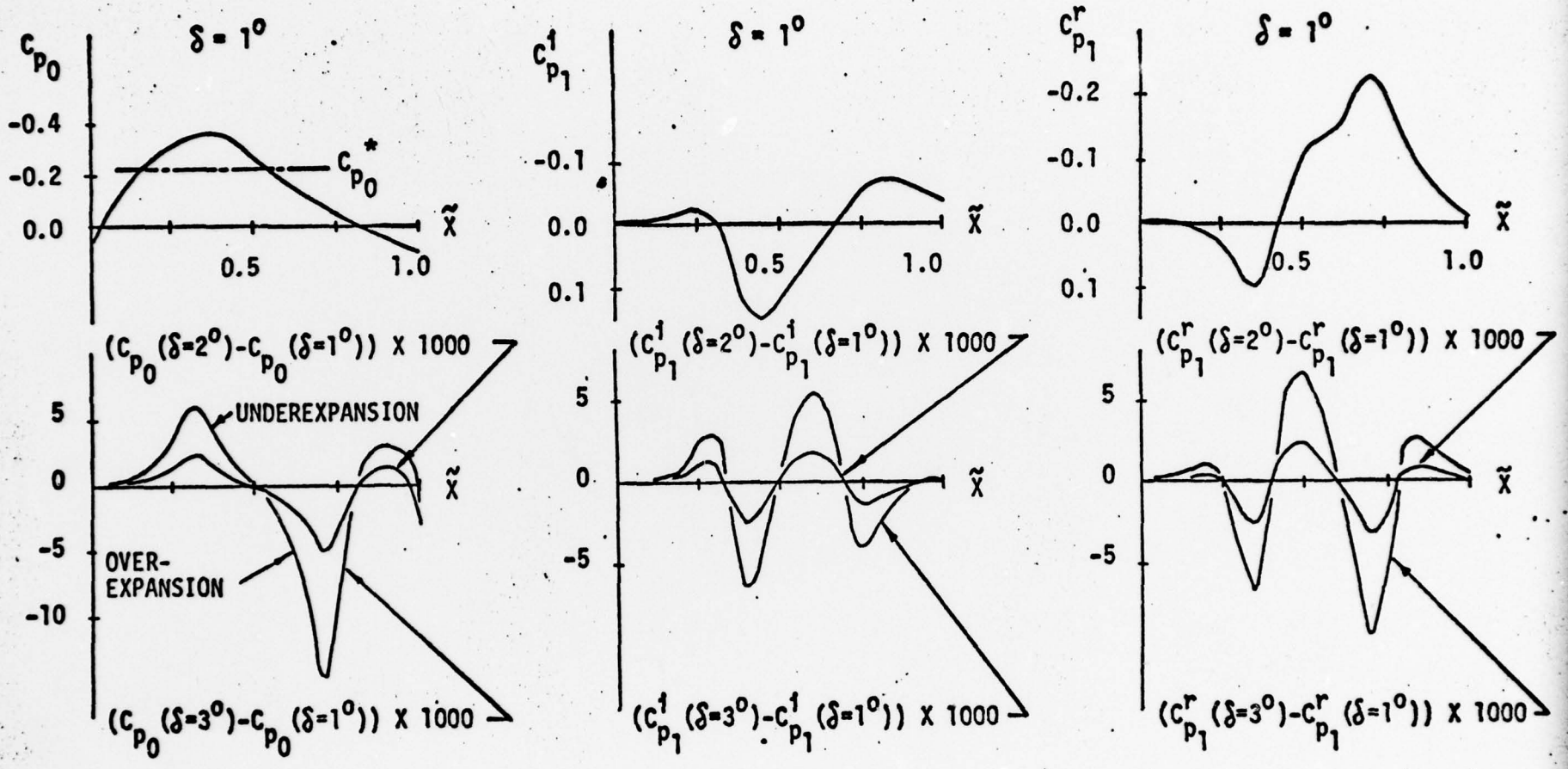

FIGURE 7. MACH 0.85, REDUCED FREQUENCY 0.24, FLAP DEFLECTIONS 1°, 2° AND 3° CASES. (NONLINEAR HARMONIC METHOD)

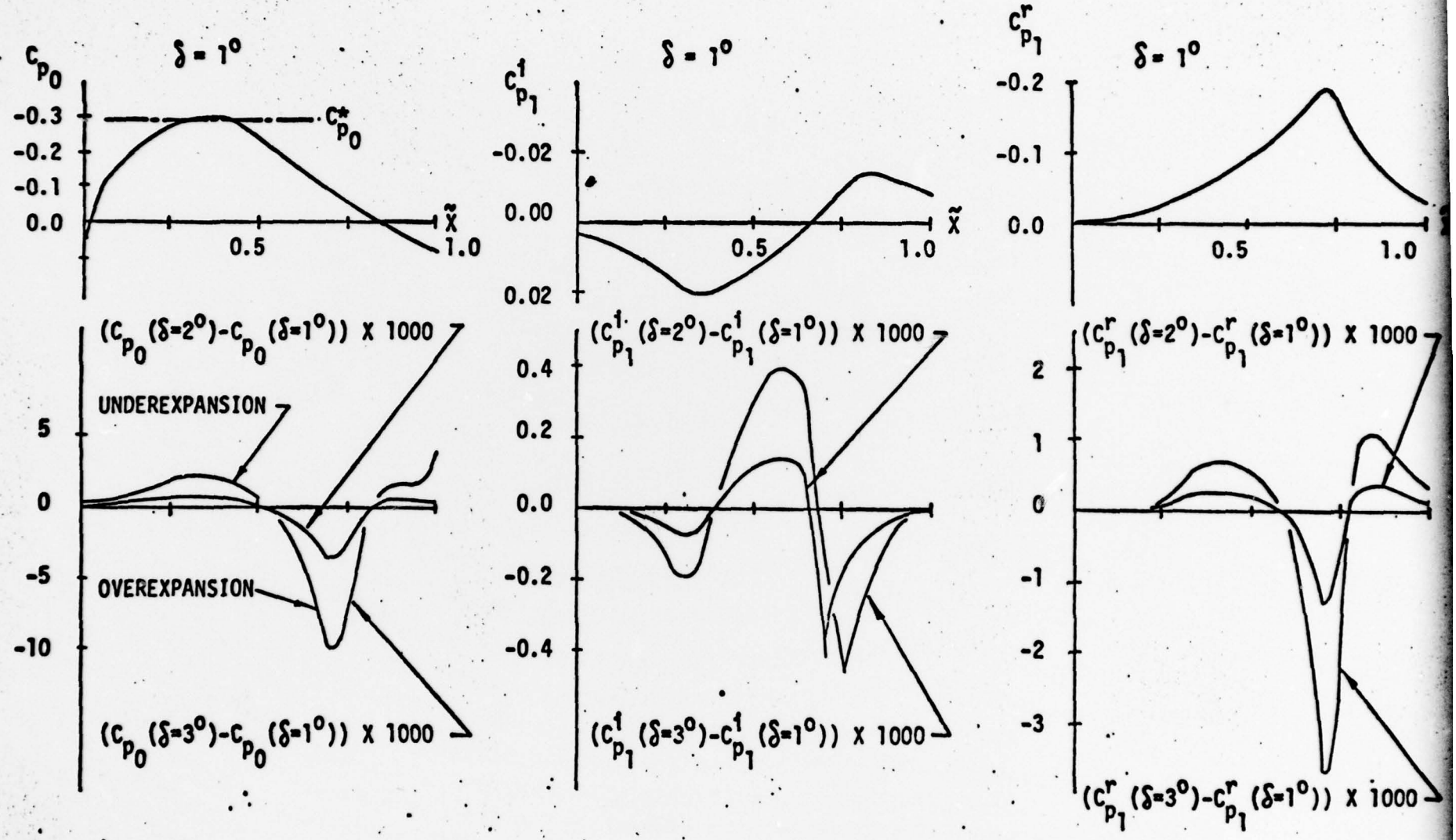

FIGURE 8. MACH 0.80, REDUCED FREQUENCY 0.064, FLAP DEFLECTIONS 1^o, 2^o AND 3^o CASES.
(NONLINEAR HARMONIC METHOD)